SEISMIC SAFETY OF CONCRETE GRAVITY DAMS BASED ON DYNAMIC CRACK PROPAGATION ANALYSIS DURING LARGE-SCALE EARTHQUAKES

H. KIMATA

Civil Engineering Division, Shimizu Corporation (Seavans South, 1-2-3, Shibaura, Minato-ku, Tokyo 105-8007 Japan), kimata@shimz.co.jp

Y. FUJITA

Engineering Division, Shimizu Corporation (Seavans South, 1-2-3, Shibaura, Minato-ku, Tokyo 105-8007 Japan), yutaka.fujita@shimz.co.jp

K. NIIMI, D. MIYAMOTO, K. NAKAYAMA, Y. USHIDA

Civil Engineering Division, Shimizu Corporation (Seavans South, 1-2-3, Shibaura, Minato-ku, Tokyo 105-8007 Japan)

ABSTRACT

Dynamic crack propagation analysis was used to assess the seismic safety of concrete gravity dams in large-scale earthquakes. Since damping characteristics have been shown to have a major effect on the occurrence and propagation of cracks in dam body, we first discuss damping characteristics by comparing existing shaking table test results with the results of dynamic crack propagation analysis. We then perform dynamic crack propagation analysis on a full-scale dam model to make clear crack occurrence and propagation during a large-scale earthquake. By performing dynamic crack propagation analysis while varying the acceleration level of the input seismic motion, we define the residual factor of ligament length as a new measure related to the crack propagation length, and we use it to perform a quantitative evaluation of seismic safety against crack penetration failure.

***Keywords*:** Concrete gravity dam, Seismic safety, Dynamic crack propagation analysis

INTRODUCTION

Current seismic design methods for dams are based on the seismic coefficient method (Ministry of Construction River Bureau (1998)). So far, none of the dams in Japan that were designed by this method have suffered any major seismic damage. Although it has been reported that large cracks were detected in the structure of several concrete dams after large-scale earthquakes in other countries (including China's Hsinfengkiang dam, India's Koyna dam, the US's Pacoima dam, and Iran's Manjil dam), the damage was not fatal in any of these cases.

On the other hand, after Hyogo-ken Nanbu earthquake in Japan in 1995, it was shown that evaluating the seismic safety of many civil engineering structures in large-scale earthquakes is very important (JSCE (2000)). The seismic coefficient method is not possible to evaluate seismic safety of the structures in a large-scale earthquake which occurrence frequency is very low in life-time of them. Thus, even in relation to dams, it is thought that seismic safety evaluation is an essential research topic for clarifying their behavior during large-scale earthquakes.

Since a concrete gravity dam is a plain concrete structure, the ultimate state under large-scale earthquakes is expected to be penetration failure resulting mainly from the occurrence and propagation of cracks in the dam body (METI and JEPOC (2001)). Various analytical studies have already looked into the propagation behavior of cracks in dam body. Factors that influence the occurrence and propagation of cracks in dam body include the input seismic motion, the amount of water in the reservoir (i.e., the water level), and tension softening characteristics of concrete and damping characteristics. In earlier studies, Zhang and Ohmachi studied the effects of the reservoir water and the penetration of water into cracks (Zhang and Ohmachi (1998); Zhang and Ohmachi (2000)), and Sasaki et al. studied how the tension softening characteristics of concrete affect properties such as the failure energy and tensile strength (Sasaki and Kanenawa (2003); Sasaki et al, (2003)).

Damping characteristics have been shown to have a particularly large effect on the occurrence and propagation of cracks in the dam bodies of concrete gravity dams. At the Ministry of Economy, Trade and Industry (METI), in order to make clear the crack propagation behavior of concrete gravity dams during large-scale earthquakes, two-dimensional FEM nonlinear dynamic analysis has been performed using a smeared crack model that takes the tension softening characteristics of the concrete into account. However, this technique has been shown to be incapable of getting the crack localization phenomenon inherent in plain concrete structures through the distribution of cracking, and there are problems involved in a damping evaluation method (METI and JEPOC (2001)). El-Aidi and Hall (1989) [1,2] showed that damping characteristics have a large effect on crack propagation behavior, and that the mass proportional parts in Rayleigh damping constitute a resisting force at the surfaces where cracks occur so that the stress release becomes insufficient. They applied stiffness-proportional damping to a nonlinear dynamic analysis. Bhattacharjee et al. (1993) and Horii and Chen (2003) also reported similar findings, and in general it is thought that crack localization phenomena can be indicated by using the initial stiffness to set the stiffness-proportional damping but employing the time-domain stiffness proportional damping that degrades from one moment to the next as cracks propagate. Also, Lee et al. (1998) evaluated the crack propagation behavior in dams by introducing a damage variable to vary the damping characteristics according to the amount of damage (the stiffness softening associated with crack propagation).

Since these studies have shown that the damping characteristics have a significant effect on the occurrence and propagation of cracks in the dam bodies of concrete gravity dams, in the present study we first investigated a suitable method for evaluating damping characteristics by comparing the results of dynamic crack propagation analysis and shaking table tests (Tinawa et al. (2000)) on plain concrete structures made to simulate existing dams. Next, we made clear occurrence and propagation of cracks in dams during large-scale earthquakes by performing nonlinear dynamic analysis of a model dam based on the largest class of concrete gravity dams in Japan. Finally, based on the knowledge gained in this way, we performed a nonlinear dynamic analysis while varying the acceleration level of the input seismic motion, and we proposed the residual factor of ligament length in relation to the crack propagation length as a new measure for quantitative evaluation of seismic safety against crack penetration failure (METI and JEPOC (2001)).

Methods for analyzing the occurrence and propagation of cracks can be broadly divided into discrete crack model and smeared crack model analysis methods. In this study we performed an analytical investigation based on two-dimensional FEM nonlinear dynamic analysis with a smeared crack model. This method is referred to as "dynamic crack propagation analysis" in the following.

1. EVALUATION OF DAMPING CHARACTERISTICS DURING THE OCCURRENCE AND PROPAGATION OF CRACKS IN DAMS

1.1. Damping characteristics evaluation method

The equation of motion used to analyze dynamic crack propagation in concrete gravity dams is shown in Eq. [1] below. In this equation, Rayleigh damping is generally used to deal with structural damping. The damping matrix of Rayleigh damping can be constituted of a mass matrix and an initial stiffness matrix as shown in Eq. [2].

$$\left[M\right]\ddot{\mathbf{u}}+\left[C\right]\dot{\mathbf{u}}+\left[K\right]\mathbf{u}=\left\{f(t)\right\} \qquad [1]$$

$$\left[C\right]=a\left[M\right]+b\left[K_0\right] \qquad [2]$$

Here, $\left[M\right]$ is the mass matrix, $\left[C\right]$ is the damping matrix, $\left[K_0\right]$ is the initial stiffness matrix, $\ddot{\mathbf{u}}$ is the acceleration vector, $\dot{\mathbf{u}}$ is the velocity vector, $\mathbf{u}$ is the displacement vector, $\left\{f(t)\right\}$ is the external force vector, and the constants a and b are determined from the first and second circular frequency and mode damping constant.

For a plain concrete structure, according to an past study in which the Rayleigh damping shown in Eq. [1] was used to study the occurrence and propagation of cracks in dams (METI and JEPOC (2001)) it has been shown that cracks become more dispersed and less liable to propagate as the damping increases, whereas cracks become localized and propagate more easily when the damping is small. Essentially, when cracks have occurred in plain concrete structures, one would expect that tensile stress will no longer propagate at the crack plane, unlike in reinforced concrete structures. However, when the damping matrix in Eq. [2] is employed in the equation of motion, when the crack opening velocity occurs orthogonal to a crack, it is accompanied by a damping force which acts as a resisting force that transmits the tensile stress so that the crack becomes liable to disperse and less likely to propagate.

Therefore, in order to represent the abovementioned characteristics as faithfully as possible, we set up a damping matrix as described below.

(i) With regard to the Rayleigh damping used for dynamic crack propagation analysis, since the existence of $\left[M\right]$ results in increased damping at low frequencies and an inability for stress to be suitably released in the regions adjacent to cracks, the effects of the damping force are eliminated when cracks occur by ignoring $a\left[M\right]$ in Eq. [2] as shown by the following formula:

$$\left[C\right]=b\left[K_0\right] \qquad [3]$$

(ii) Furthermore, $\left[K_0\right]$ is not treated as a matrix consisting of constant elements, but as a matrix that varies as a function of time *t* as follows:

$$\left[C(t)\right]=b\left[K(t)\right] \qquad [4]$$

Here, $\left[C(t)\right]$ is the damping matrix depended on time *t*, $\left[K(t)\right]$ is the stiffness matrix at time *t*, and *b* is a constant determined by the first circular frequency and mode damping constant. In other words, by applying damping that varies according to the constantly varying stiffness $\left[K(t)\right]$, the stiffness becomes zero and no damping forces occur the crack plane when a crack has become fully open. The damping in this way has the effect of making the transmission of tensile stress at crack surfaces coincident with the actual transmission when cracks occur and propagate.

In the next section, we compare the results of large-scale shaking table tests on plain concrete structure of dam shape and the results of dynamic crack propagation analysis performed using Eqs. [3] and [4], and we investigate how the damping characteristics affect the occurrence and propagation of cracks.

1.2 Verification of existing methods for evaluating damping characteristics based on shaking table tests

Tinawi et al. (2000) used a shaking table to perform acceleration tests on a plain concrete structure shaped on a concrete gravity dam. A schematic view of the structure they tested is shown in Figure 1. This structure was 3.4 m high with a downstream gradient of 0.7, and was 0.25 m thick. To reduce the natural frequency of the test piece, an additional mass of 2700 kg was placed on top. To limit the places where cracks could occur, notches were provided in the upstream and downstream sides. To achieve a compressive strength of about 15 MPa, the test piece was made using concrete with a high water-cement ratio. At the foundation fixtures of this test piece, the first circular frequency was 21.8 Hz, and the combined natural frequency with the shaking table was 16.4 Hz. The input waves applied to this test structure had three types of pulse wave, and the shaking table was vibrated intermittently with three jolts. From the control performance of the shaking table, the acceleration obtained from the shaking table became almost sinusoidal as shown in Figure 2. According to the test results, the first jolt did not cause any cracks to form in the dam body, but a crack formed in the downstream side of the dam body at the second jolt. Then, at the third jolt, a crack propagated from the upstream side to the downstream side, resulting in penetration failure. Figure 3 shows the state of crack propagation resulting from the second and third jolts.

Next, Tinawi et al. (2000) subjected this structure to dynamic crack propagation analysis. They used stiffness-proportional damping in their analysis, and to avoid tensile stresses occurring to the cracks, damping was deliberately not considered in the elements where cracks occurred. However, the crack paths obtained from

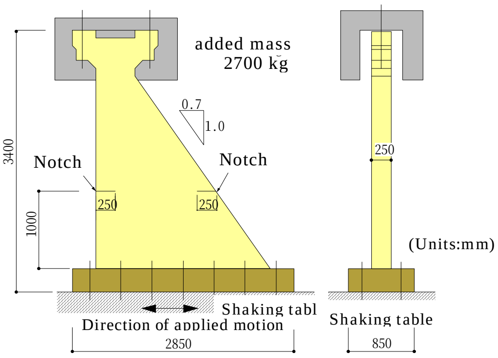

Figure 1. Outline of test structure (Tinawa et al. (2000))

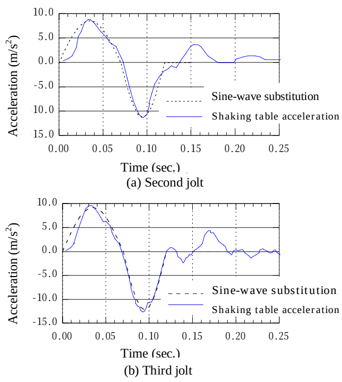

Figure 2. Input pulse wave, Taniwa et al. (2000)

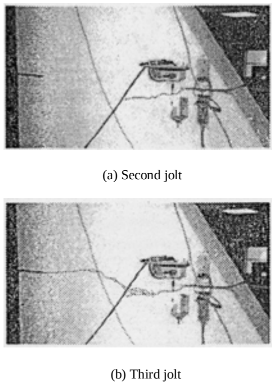

Figure 3. Crack propagation state, Taniwa et al. (2000)

the analysis only ran horizontally between the notches, so the crack paths obtained from the experimental results could not be suitably represented. They did not adequately explain this issue, and the factors that caused the discrepancy between the two sets of results are not clear.

On the other hand, the authors have performed a dynamic crack propagation analysis based on the damping characteristics evaluation method described in the previous section. The analysis model is shown in Figure 4. The structure was modeled assuming a plane stress state, and to prevent snap-back it was partitioned into a mesh of triangular elements based on an equilateral triangle with a side of length 0.05 m (crack band width: 0.05 × sin 60° m). We used the same analytical constants as those used by Tinawi et al., which are shown in Table 1. For the relationship between the tensile stress and crack opening displacement, we used the bilinear type of constitutive model of tension softening (1/4 model) shown in Figure 5 (Rokugo et al. (1989)). In the relationship between the tensile stress and crack opening displacement, we set an origin-oriented hysteresis characteristic during unloading. We also assumed that concrete behaves as linear elastic solid under compression. The coefficient of shear stiffness reduction after the occurrence of cracking was set to 0.005, and the Newton-Raphson method was used with the convergence decision evaluated by the energy norm (convergence error 10^{-4}).

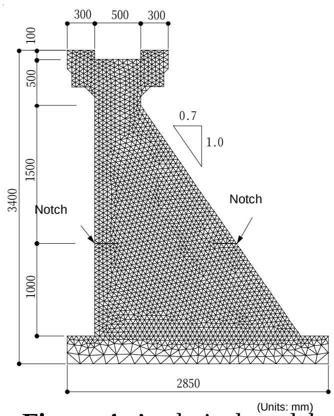

Figure 4. Analytical model

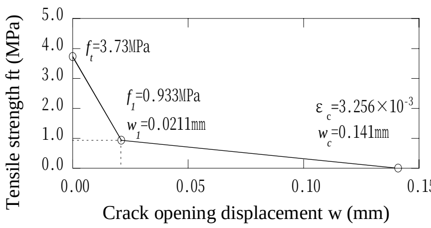

Figure 5. Constitutive model of concrete tension softening

Table1. Dynamic properties of concrete (Tinawi et al. (2000))

Constant	Value
Compressive strength f_c (MPa)	14.8
Tensile strength ft (MPa)	3.7
Young's modulus E (GPa)	18.5
Poisson ratio ν	0.19
Density ρ (kg/m3)	2400
Failure energy Gf (N/m)	105

Note: These constants were used in a study by Tinawi

With regard to the damping of the concrete test structure, we applied the two types of damping mentioned in the previous section (one proportional to the time-domain stiffness, the other proportional to the initial stiffness), and the damping constant of the first natural mode of the test structure was assumed to be 2.5%. According to the eigenvalue analysis results of the concrete test structure, the first natural frequency f_1 was 16.4 Hz, and the value of constant b ($=h_1/\pi f_1$) in Eqs. [3] and [4] was 4.85×10^{-4}.

Figure 2 shows the input acceleration wave applied to the test structure. The acceleration wave used in the analysis was a sinusoidal wave adjusted so that the period and the positive/negative peaks matched the acceleration wave generated by the shaking table, and only one period of the main wave was considered.

Figures 6 through 9 show the crack opening strain distribution and the maximum principal stress distribution during the application of the second and third pulse wave in this analysis. The crack opening strain distribution shows the region in which cracks occur, and the results of analysis using time-domain stiffness proportional damping correspond very closely to the cracks that occurred in the test as shown in Figure 3. Also, from the maximum principal stress distribution it appears that the tensile stress was released the crack, suggesting that we were able to suitably reproduce the crack propagation phenomenon. On the other hand, when using initial stiffness proportional damping, the damping affected the tensile stress to the crack even after the crack had generated, so that the crack did not grow much and it was not possible to reproduce the phenomenon.

It is therefore concluded that when reproducing the generation and propagation of cracks in concrete gravity dams, it is better to use time-domain stiffness proportional damping as shown in Eq. [4].

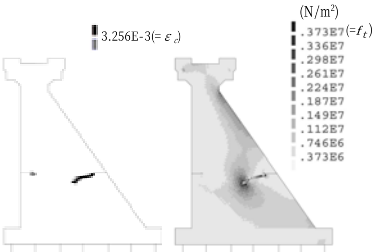

(a) Crack opening (b) Maximum principal stress

Figure 6. Crack opening strain distribution and maximum principal stress distribution during the second jolt (time-domain stiffness proportional damping)

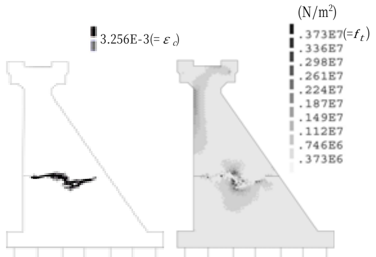

(a) Crack opening (b) Maximum principal stress

Figure 7. Crack opening strain distribution and maximum principal stress distribution during the third jolt (time-domain stiffness proportional damping)

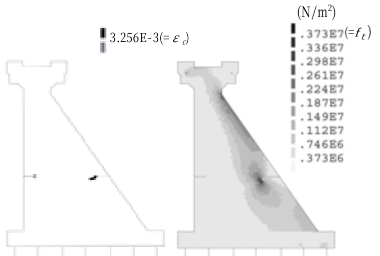

(a) Crack opening (b) Maximum principal stress

Figure 8. Crack opening strain distribution and maximum principal stress distribution during the second jolt (damping proportional to the initial stiffness)

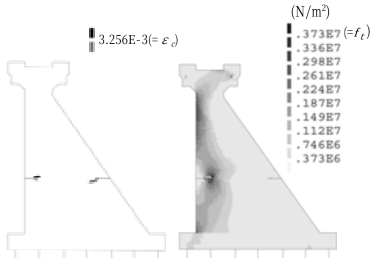

(a) Crack opening (b) Maximum principal stress

Figure 9. Crack opening strain distribution and maximum principal stress distribution during the third jolt (damping proportional to the initial stiffness)

2. GENERATION AND PROPAGATION OF CRACKS IN DAMS

We performed a dynamic crack propagation analysis using a model of the largest class of concrete gravity dam in Japan (height: 150 m), and we investigated the crack propagation behavior in concrete gravity dam bodies during large-scale earthquakes.

2.1 Analysis conditions

2.1.1 Analysis model

The analysis model is shown in Figure 10. The dam was assumed to be subjected to a plane strain in the direction perpendicular to the dam axis (the upstream/downstream direction), and two-dimensional FEM was performed dynamic crack propagation analysis using the model comprising the dam body, foundation bedrock and reservoir water.

To prevent snap-back in the dynamic crack propagation analysis, the dam structure was divided into a mesh of triangular elements based on an equilateral triangle with a side of length 1.95 m (crack band width = 1.95 × sin 60° m). The foundation bedrock was modeled over a region extending over about 8.3 times the width of the dam at the base (1136.8 m), and to a depth of twice the dam body height (300 m). The bottom surface of the model was provided with dashpots simulating a semi-infinite boundary to allow the dissipation of seismic waves to be taken into account. Free ground was provided at the sides of the model with dashpots to transmit energy to the free ground, thereby allowing the dissipation of seismic waves to be taken into consideration in a similar manner. The reservoir water was treated as an additional mass determined from Westergaard's formula (Westergaard (1933)).

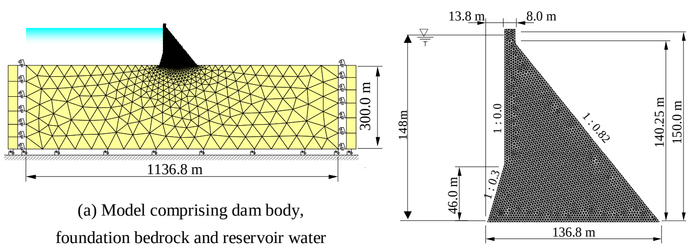

(a) Model comprising dam body, foundation bedrock and reservoir water

(b) Dam structure

Figure10. Analytical model

2.1.2 Analytical constants

The main analytical constants of the model dam are shown in Table2. These values were set by referring to past studies, including those of the METI and JEPOC (2001), the CEB (1993), and Horii et al. (2000)

We used the bilinear type of concrete tension softening constitutive model (1/4 model) (Rokugo, 1989) to simulate the relationship between tensile stress and crack opening displacement in the concrete of the dam structure (see Figure 11), and an origin-oriented hysteresis characteristic was assumed during unloading. Also, with regard to the concrete compression characteristics, we used the Drucker-Prager failure criterion (Drucker and Prager (1952)) to take account of nonlinearities, and we used a coefficient of 0.005 for the reduction of shear stiffness after crack formation. The foundation bedrock was assumed to be linear elastic solid. The Newton-Raphson method was used with the convergence decision evaluated by the energy norm (convergence error 10^{-4}).
With regard to the damping constant, the first natural mode damping h_1 was assumed to be 7% and 2% for the dam structure and the foundation bedrock respectively. According to the eigenvalue analysis results, the first natural frequencies f_1 of the dam structure and foundation bedrock were 1.43 Hz and 0.987 Hz respectively, and the values of the abovementioned constant b in Eq. [4] ($=h_1/\pi f_1$) were 1.56×10^{-2} and 6.45×10^{-3}.

Table 2. Dynamic properties of concrete and bedrock

Constant	Dam structure	Foundation bedrock
Young's modulus E (GPa)	23 (21)	10 (10)
Poisson ratio ν	0.19 (0.19)	0.25 (0.25)
Density γ (kg/m3)	2400 (2400)	2500 (2500)
Compressive strength fc (MPa)	21.0	—
Tensile strength ft (MPa)	2.1	—
Tensile energy G_f (N/m)	365	—
First-order mode damping constant h_1	0.07	0.02

Note: The numbers in brackets are the analytical constants of the initial stress analysis

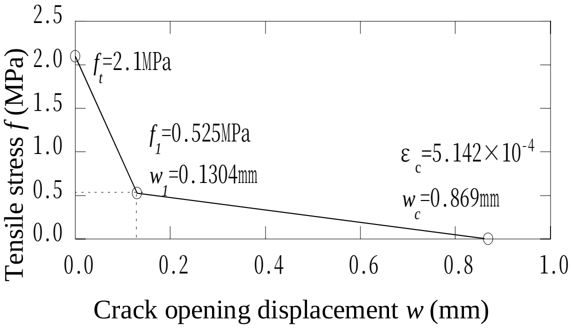

Figure 11. Constitutive model of concrete tension softening

2.1.3 Input seismic motion

To simulate the response of a large-scale earthquake, the input seismic motion used in the dynamic crack propagation analysis was designed by assuming the occurrence of a magnitude M8.0 earthquake near the site of the dam (epicentral distance Δ=25 km). An M8.0 is decided by Nobi earthquake of 1891, which was the highest magnitude known to have occurred in Japan. A response spectrum was defined at the bedrock surface, and the simulated seismic motion was made by using this as the target spectrum called Osaki spectrum (JEA (1987)).
The simulated seismic motion we used is shown in Figure 12. This corresponds to the seismic motion at the bedrock surface, and in the analysis we decided to use the input seismic motion brought down to the bottom of the model in the horizontal direction. Seismic motion in the vertical direction was dealt with using the static vertical seismic intensity kv, and by converting half of the maximum simulated seismic motion of 5.74 m/s^2 in the horizontal direction into the seismic intensity, we decided to apply $kv = 0.293$ to the analytical model in the vertical direction.

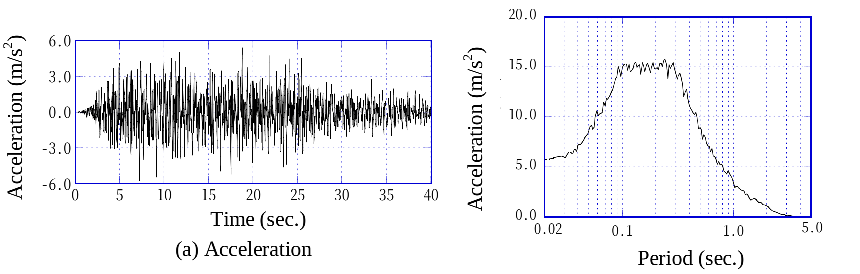

(a) Acceleration

(b) Acceleration response spectrum

Figure 12. Input motion

2.2 Analysis results

Prior to the dynamic crack propagation analysis, we conducted static analysis to get an initial stress taking into account the dead weight of the dam structure, the dead weight of the foundation bedrock, the static pressure of the reservoir water, and the uplift pressure on the bottom surface of the dam body.
The results of the dynamic crack propagation analysis are shown in Figure 13, which depicts relative displacement between the top and bottom of the dam body. Figures 14 and 15 show the crack opening strain distribution and the maximum principal stress distribution at representative times indicated in Figure 13.
From the crack opening strain distribution shown in Figure 14, it can be seen that a crack initially progressed a long way from the upstream side to the downstream side at the lower surface of the dam body, and that another crack then progressed a long way from the top of the fillet on the upstream side down towards the downstream side. When the crack starts to grow from the top of the fillet, the progress of the other crack at the bottom is suppressed. The fillet, which is provided to improve the safety of the dam body with regard to slipping and overturning, acts to induce cracking, and when a fillet is situated in a dam body it is thought to be important to give full consideration from the viewpoint of the occurrence and propagation of cracks.

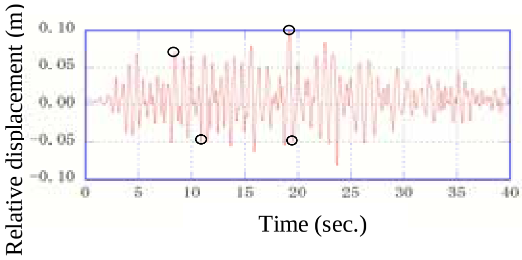

Figure 13. Relative displacement between top and bottom of the dam body

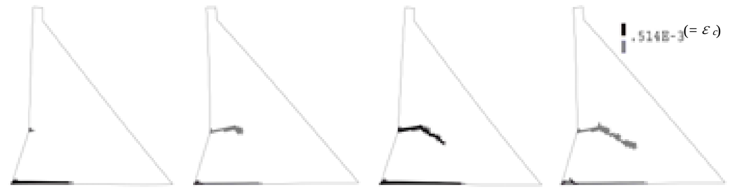

(a) t=8.4seconds (b) t=10.9seconds (c) t=19.2seconds (d) t=19.5seconds

Figure 14. Crack opening strain distribution

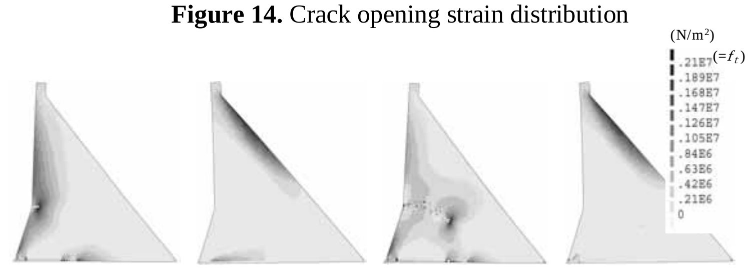

(a) t=8.4seconds (b) t=10.9seconds (c) t=19.2seconds (d) t=19.5seconds

Figure 15. Maximum principal stress distribution

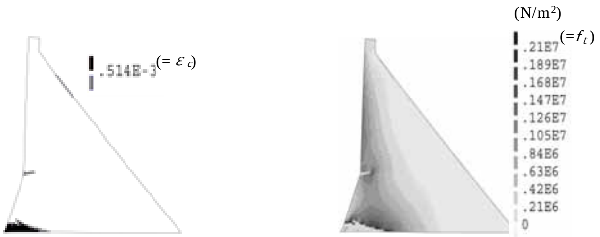

(a) Crack opening strain distribution (b) Maximum main stress distribution

Figure 16. The crack opening strain distribution and maximum principal stress distribution obtained with damping proportional to the initial stiffness (t=19.2seconds)

From the maximum principal stress distribution shown in Figure 15, especially the distribution at 19.2 seconds, it can be seen that large tensile stress only occurs at the tip of an active crack, and that the stress is fully released along the rest of the crack path and the vicinity thereof. By way of reference, Figure 16 shows the analysis results obtained at 19.2 seconds when using damping proportional to the initial stiffness under the same conditions. Here it can be seen that the stress is not fully released in the region next to the crack, and that the cracks become dispersed and progress for a shorter distance. It is thus judged that the results of this analysis can suitably show the crack propagation behavior in real concrete gravity dams when performed with time-domain stiffness proportional damping.

3. EVALUATING THE SEISMIC SAFETY OF DAMS

We subjected the abovementioned model dam to dynamic crack propagation analysis while varying the acceleration level of the input seismic motion, and we evaluated its seismic safety against crack penetration failure based on the ultimate state of the dam. As a new indicator that means the soundness of a dam against crack penetration failure, we propose using the residual factor of ligament length as expressed by the following formula (see Figure 17), and we used it to perform a quantitative assessment of seismic safety (METI and JEPOC (2001)).

$$RF_i = l_{Ri} / L_i \cdot 100 \qquad [5]$$

Here, RF_i (%) is the residual factor of ligament length for crack path i, L_i is the total length to which crack path i is expected to grow, and l_{Ri} is the length of the residual path in crack path i where cracking did not occur (the ligament length).

The crack propagation analysis of models dams was performed under the same conditions as the abovementioned analysis. For the input seismic motion, we produced different levels of seismic motion by multiplying the simulated seismic motion shown in Figure 3 (maximum acceleration 5.74 m/s^2) by factors of 0.5, 0.7, 0.8, 0.9, 1.0 and 1.05.

The analytical results are shown in Figure 18, which depicts the relationship between the residual factor of ligament length and the maximum input acceleration. Two separate relationships were determined for the crack paths propagating along the bottom of the dam body and from the top of the fillet. Here, the minimum acceleration at which cracks start to occur was determined from the relationship between the linear analysis results and the tensile strength of the concrete in the dam body. This resulted in the following findings:

(i) The residual factor of ligament length RF_1 of the crack path traveling at the bottom of the dam body decreased in a more or less linear fashion as the maximum input acceleration A_{max} increased up to about 4.5 m/s^2, where the residual factor of ligament length was about 50%.

(ii) The residual factor of ligament length RF_2 of the crack path traveling from the top of the fillet remained at 100% as the maximum input acceleration A_{max} increased up to about 4.0 m/s^2, but decreased rapidly once the crack had formed. In the region where A_{max} exceeds 5.0 m/s^2, it is smaller than the residual factor of ligament length RF_1 of the crack at the bottom of the dam body and decreases rapidly whereas RF_1 hardly changes at all. By A_{max}=5.74 m/s^2, RF_2 has fallen to 30%, and at 6.02 m/s^2 RF_2 becomes 0%, which means that the crack traveling from the top of the fillet joins up with the crack at the bottom, resulting in penetration failure. Accordingly, it was ultimately the crack path traveling from the top of the fillet that turned out to be the decisive factor with regard to crack penetration failure.

(iii) The soundness of this dam against crack penetration failure was evaluated from the envelope curves of small values of the residual factors of ligament length RF_1 and RF_2 of cracks in the bottom and fillet parts. When the maximum input acceleration A_{max} is about 4.5 m/s^2, the residual factor of ligament length RF is about 50%, and at values of up to about 4.5 m/s^2, the soundness decreases in a roughly linear fashion as described above. However, at higher accelerations the soundness decreases sharply. When A_{max}=5.74 m/s^2, the value of RF is only about 30%, and at 6.02 m/s^2 it reaches 0%, leading to penetration failure. Accordingly, to ensure the seismic safety of dams, it is thought that one desirable target is to keep the residual factor of ligament length to about 50% or less.

(iv) The simulated seismic motion of magnitude M8.0 assumed in this study is thought to correspond to the movement of the largest class of large-scale earthquake liable to occur directly beneath a dam site. However, even with this level of seismic motion, crack penetration failure does not occur if the residual factor of ligament length RF is about 30%, thus ensuring the seismic safety of the dam.

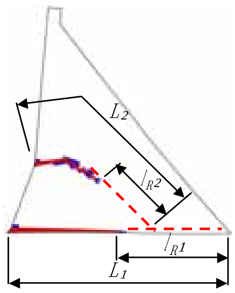

Crack path	Residual factor of ligament length RF_i (%)
Bottom	$RF_1 = l_{R1} / L_1 \cdot 100$
Fillet	$RF_2 = l_{R2} / L_2 \cdot 100$

Figure 17. Residual factor of ligament length

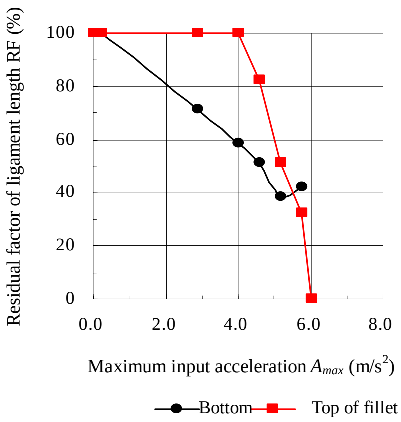

Figure 18. Relationship between residual factor of ligament length and maximum acceleration

4. CONCLUSION

We have performed dynamic crack propagation analysis to evaluate the seismic safety of a concrete gravity dam during a large-scale earthquake. By focusing on the fact that the damping characteristics affect the occurrence and propagation of cracks in the dam structure, we investigated a suitable method for evaluating the damping characteristics. We then investigated cracks occur and propagate in a full-scale dam model, and we attempted to quantitatively evaluate its seismic safety. Findings from present study can be summarized as follows:

(i) Using the results of earlier shaking table tests of plain concrete structures simulating concrete gravity dams, we investigated a method for evaluating the damping characteristics by applying dynamic crack propagation analysis. As a result, by employing the damping matrix shown in Eq. [4], in which the damping is proportional to the time-domain variable stiffness matrix, we found that it is possible to release the unnecessary damping forces that actual phenomena can be suitably expressed.

(ii) Using time-domain stiffness proportional damping as studied in (i), we performed dynamic crack propagation analysis on a model dam with a dam body height of 150 m incorporating a fillet, and we investigated the occurrence and propagation of cracks in this structure. As a result, we found that cracks occur at the bottom of the dam body and from the region where the cross-section changes abruptly at the top of the fillet. This shows that the fillet, which was provided in order to improve the safety of the dam body with regard to sliding and overturning, tends to induce cracking. When a fillet is situated in a dam body, it is therefore important to fully consider the aspects of crack occurrence and propagation.

(iii) We performed dynamic crack propagation analysis on a model dam while varying the acceleration level of the input seismic motion, and we tried using the residual factor of ligament length as expressed by Eq. [5] to evaluate the seismic safety with regard to crack penetration failure in the ultimate state of the dam. As a result, we found that when the residual factor of ligament length is less than about 50% with a maximum input acceleration of about 4.5 m/s^2, the dam structure approaches crack penetration failure very rapidly as the maximum input acceleration increases. This suggests that in order to ensure the seismic safety of a dam, one target should preferably be to keep the residual factor of ligament length to about 50% or more.

(iv) We have confirmed that even when a large-scale earthquake of magnitude M8.0, which is the largest class of earthquake, occurs directly below the dam site, no crack penetration failure occurs and the dam remains safe when the residual factor of ligament length is about 30%.

In the future, we plan to evaluate the seismic safety of concrete gravity dams with lower dam body by subjecting them to the same kind of analysis. We also plan to conduct investigations into other issues such as the three-dimensional effects of concrete gravity dams, the effects of water that penetrates into cracks that form during earthquakes, the effects of aftershocks, and earthquake-resistant strengthening methods.

ACKNOWLEDGEMENTS

I express my sincere thanks to Professor HIDEYUKI HORII, Department of Civil Engineering, University of Tokyo, whose comments and suggestions were of inestimable value for this study.

REFERENCES

Bhattacharjee, S.S. & Léger, P. (1993), "Seismic cracking and energy dissipation in concrete gravity dams", *Earthquake Engineering and Structural Dynamics*, Vol. 22, pp. 991–1007.

CEB Comite Euro-International du Beton (1993), *CEB-FIP Model Code 1990*, Bulletin d'Information, No. 213/214, pp. 36–37.

Drucker, D.C. & Prager, W. (1952), "Soil mechanics and plastic analysis or limit design", *Q. Appl. Math.*, Vol. 10, No. 2, pp. 157–165.

El-Aidi, B. & Hall, J.F. (1989), "Non-linear earthquake response of concrete gravity dams, Part 1: Modelling", *Earthquake Engineering and Structural Dynamics*, Vol. 18, pp. 837–851.

El-Aidi, B. & Hall, J.F. (1989), "Non-linear earthquake response of concrete gravity dams, Part 2: Behaviour", *Earthquake Engineering and Structural Dynamics*, Vol. 18, pp. 853–865.

Horii, H. & Chen, S.C. (2003), "Computational fracture analysis of concrete gravity dams by crack-embedded elements-toward an engineering evaluation of seismic safety", *Engineering Fracture Mechanics*, No. 70, pp. 1029–1045.

Horii, H., Uchida, Y., Kashiwayanagi, M., Kimata, H. and Okada, T. (2000), "Investigation of tension softening characteristics for evaluating the strength of concrete dams", *JEPOC*, No. 286.

Japan Electric Association (JEA) (1987), *Technical guidelines for the quake-proof design of nuclear power stations*, JEAG4601-1987 (In Japanese).

Japan Society of Civil Engineers (JSCE) (2000), *Proposals regarding the quake resistance of civil engineering structures (third proposal)*, JSCE (In Japanese).

Lee, J. & Fenves, G.L. (1998), "A plastic-damage concrete model for earthquake analysis of dams", *Earthquake Engineering and Structural Dynamics*, Vol. 27, pp. 937–956.

Ministry of Construction River Bureau and the Japan River Association (1998), *Ministry of Construction technical standard for controlling river erosion (draft) Explanatory section*, Design edition [I] (In Japanese).

Ministry of Economy, Trade and Industry (METI) and Japan Electric Power Civil Engineering Association (JEPOC) (2001), *Report on an investigation into improving the quake resistance of dam designs, 2000 report on quake-proof measures for electrical power facilities (quakeproof reliability proof testing of power generating facilities)* (In Japanese).

Rokugo, K., Iwasa, M., Suzuki, T. and Koyanagi, W. (1989), "Testing methods to determine tensile strain softening curve and fracture energy of concrete", *fracture toughness and fracture energy*, Balkema, pp. 153–163.

Sasaki, T. & Kanenawa, K. (2003), "Evaluation of the quake resistance of concrete dams to large (level 2) seismic motion", *Civil Engineering Journal*, Vol. 45, No. 4, pp. 10–11 (In Japanese).

Sasaki, T., Kanenawa, K. and Yamaguchi, Y. (2003), "A numerical study of crack propagation in concrete gravity dams during large-scale earthquakes", *Civil Engineering Journal*, Vol. 45, No. 6, pp. 60–67 (In Japanese).

Tinawi, R., Léger, P., Leclerc, M. and Cipolla, G. (2000), "Seismic safety of gravity dams, From Shake Table experiments to numerical analysis", *Journal of Structural Engineering*, pp. 518–529.

Westergaard, H.M. (1933), "Water Pressures on dams during earthquakes", *Trans. ASCE*, Vol. 75, pp. 418–433.

Zhang, H. & Ohmachi, T. (1998), "2-dimensional analysis of seismic cracking in concrete gravity dams", *Dam Engineering*, Vol. 8, No. 2, pp. 93–101.

Zhang, H. & Ohmachi, T. (2000), "Seismic cracking and strengthening of concrete gravity dams", *Dam Engineering*, Vol. 10, No. 3, pp. 232–240.